Gold Bulletin (2020) 53:39–46
https://doi.org/10.1007/s13404-020-00272-3

ORIGINAL PAPER

A new route for developing highly efficient nano biochemical sensors for detecting ultra-low concentrations of tetracycline antibiotic residue in water

Alwan M. Alwan[1] · Layla A. Wali[2] · Khulood K. Hasan[2]

Received: 15 October 2019 / Accepted: 8 January 2020 / Published online: 10 March 2020

Abstract
This study reports a new detection process for sensing ultra-low concentrations of tetracycline (TC), using a hot spot surface-enhanced Raman scattering (SERS) sensor. A gold nanoparticles/ macroporous silicon (Au NPs/macroPSi) hot spot SERS sensor was fabricated using a very simple and low cost method. The SERS signal was investigated using Au NPs/macroPSi hot spot SERS sensor for efficient detection of TC antibiotics at lower concentrations of (10^{-3}–10^{-9}) mol/L. The sensor showed an excellent performance for TC detection with an enhancement factor (EF) of 2×10^8, ultra-low detection limit of 10^{-9} mol/L, and very high reproducibility with a relative standard deviation of 2%. The effect of the pH value on the behavior of the SERS spectra for TC antibiotic was evaluated, and it was found that pH values of 5 and 6 were the best for the detection process of TC antibiotic.

Keywords SERS · Hot spot regions · Gold nanoparticles · Macroporous silicon · Tetracyclines

Introduction

Tetracyclines are an important class of antibiotics that consist of a broad-spectrum of members, including doxycycline, methacycline, minocycline, oxytetracycline, chlortetracycline, and tetracycline (TC) [1, 2]. They exhibit activity against a wide variety of microorganisms (e.g., gram-positive and gram-negative bacteria, atypical organisms such as rickettsiae, mycoplasmas, and chlamydiae, and protozoan parasites) [3]. They are extensively used as medicine for deterrence of bacterial contagions in humans, animals, and plants, and as growth promoters in the feeds of the poultry, animals and fishes [4]. Due to their wide usage, teracyclines residues have been found in soil, groundwater, surface water, and drinking water [5], and due to their high aqueous solubility and their long environmental half-life, the residues of tetracyclines may develop bacteria resistant strains. The resulting health problems (e.g., allergy, liver toxicity, central nervous system and gastrointestinal system, nephrotoxicity, and adverse reactions of blood system) are serious issues [6, 7], that demand more attention to conform to environmental safety requirements.

Several studies have been done to develop the detection of tetracycline antibiotic by using different methods, such as, high-performance liquid chromatography (HPLC) [8], enzyme-linked immunosorbent assay (ELISA) [9], chemiluminescence (CL) [10], microbiological methods (MM) [11], capillary electrophoresis (CE) [12], antibody-based electrochemical biosensors [13], fluorescence-based assays [14], and immunoassay (IA) [15]. These methods have many drawbacks, such as their complexity, cost, and laborious nature [16].

Plasmonic nanoparticles (NPs) such as Ag NPs and Au NPs have shown new possibilities for the development of the antibiotic detection methods because of its unique optical properties such as localized surface plasmon resonance (LSPR) [17–20]. The LSPR is a coherent oscillation of free electrons on the surface of plasmonic NPs excited by the incident wave light trapped

✉ Alwan M. Alwan
alkrzsm@yahoo.com

[1] Department of Applied Sciences, University of Technology, Baghdad, Iraq

[2] Department of Science, College of Basic Education, Mustansiriyah University, Baghdad, Iraq

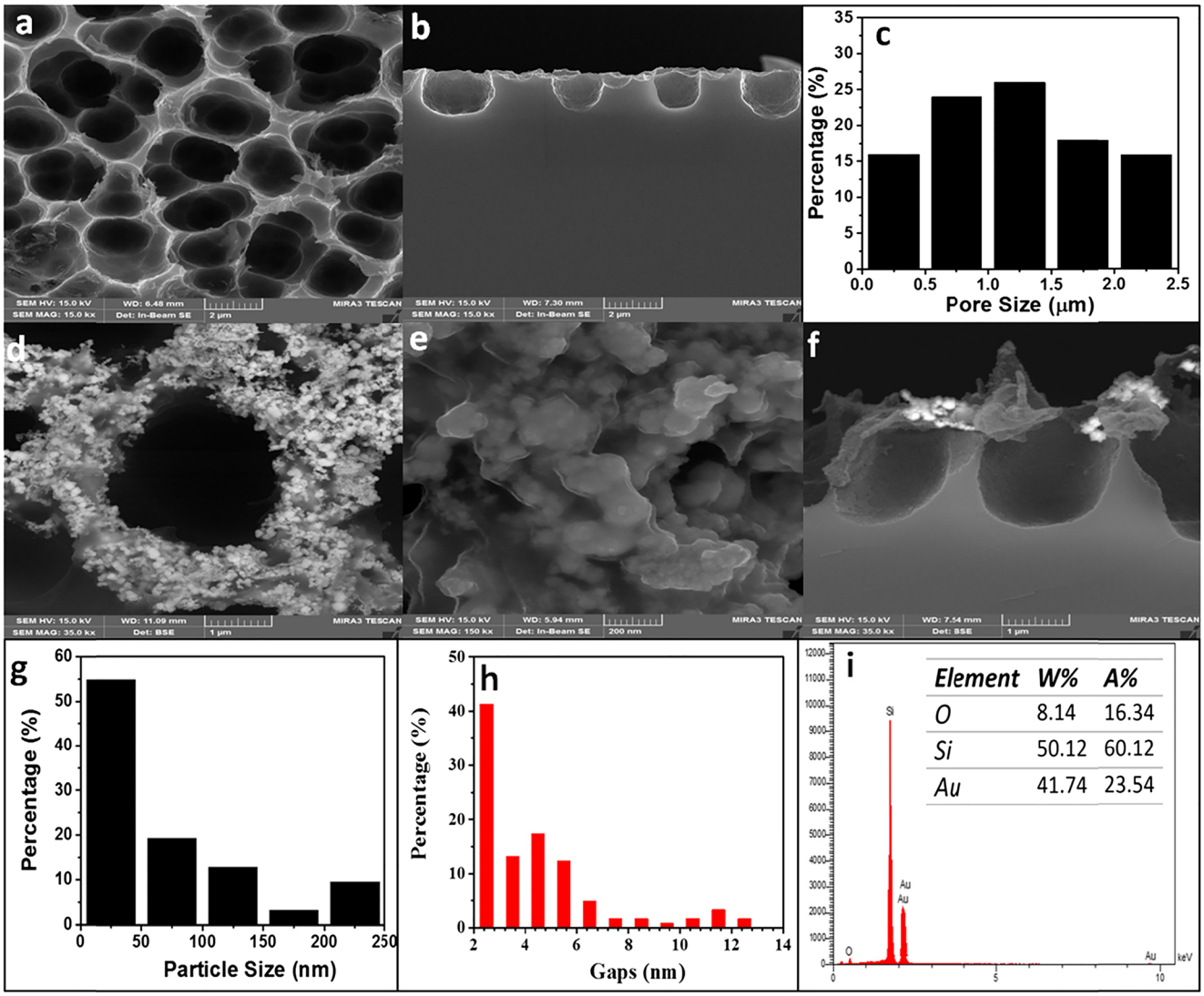

Fig. 1 **a** The FE-SEM of the bare macroPSi surface morphology, (**b**) cross-sectional FE-SEM image of macroPSi surface, (**c**) the statistical distribution of pore sizes of macroPSi substrate, (**d**, **e**) FE-SEM image of the Au NPs/macroPSi hot spot sensor at magnification of 1 μm and 200 nm, respectively, (**f**) cross-sectional FE-SEM image of Au NPs/macroPSi hot spot sensor, (**g**) the statistical distribution of particle sizes and (**h**) the distance among them, and (**i**) EDS analysis of this sample

within plasmonic NPs that are smaller than the incident light wavelength [21].

The localized electric field intensity of the LSPR of metallic NPs can be enhanced by increasing the density of hot spots, which play a major role in the surface-enhanced Raman scattering (SERS) [22]. The Au NPs aggregates more favorable choices for developing SERS because they have higher density of hot spots. The Au NPs can be synthesized on the surface of macroporous silicon (macroPSi) with a higher density of hot spot regions owing to high density of nucleation sites of the macroPSi layer [23, 24]. In this study, new route was innovated for developing high efficient nano biochemical sensor for sensing ultra-low concentration of TC antibiotics, based on the enhanced plasmonic properties of Au NPs deposited on the macroPSi substrate.

Experimental section

Chemicals

Chloroauric acid ($HAuCl_4$, 99.99%), tetracycline hydrochloride ($C_{22}H_{24}N_2O_8$ HCl, 96%), and ethanol (C_2H_5OH, 99.98%) were purchased from Sigma-Aldrich, Germany. Hydrofluoric acid (HF, 40%) was purchased from HiMedia, India.

Preparation of macroPSi substrates

The MacroPSi substrates were obtained by a photo-electrochemical etching process at room temperature. A 100-single-polished silicon wafer with resistivity of 10 Ω cm was divided into square pieces with an area of 2.25 cm^2. These

pieces were cleaned for several minutes using a solution of HF and ethanol mixed in a volume ratio of (1:10) to remove the native oxide which found on the Si piece surfaces, and then washed with ethanol. The piece of Si wafer was placed in a teflon cell to form an anode electrode, and a platinum ring was immersed in a mixture HF:ethanol = 1:1 to form a cathode electrode. An area of 0.6 cm^2 of the Si surface was illuminated with light from a CW diode laser of 30 mW/cm^2 power density and 630-nm wavelength. The etching process was performed for 20 min with a current density of 50 mA/cm^2. The macroPSi substrates were prepared with a high surface density of dangling bonds (Si-H) by controlling the etching conditions.

Deposition process of Au NPs

The dipping process of macroPSi substrates into aqueous solution of 10^{-3} M $HAuCl_4$ and 3 M HF was used to prepare the aggregate of Au NPs. The dipping process was done at room temperature with a 3 min dipping time. The Au NPs were

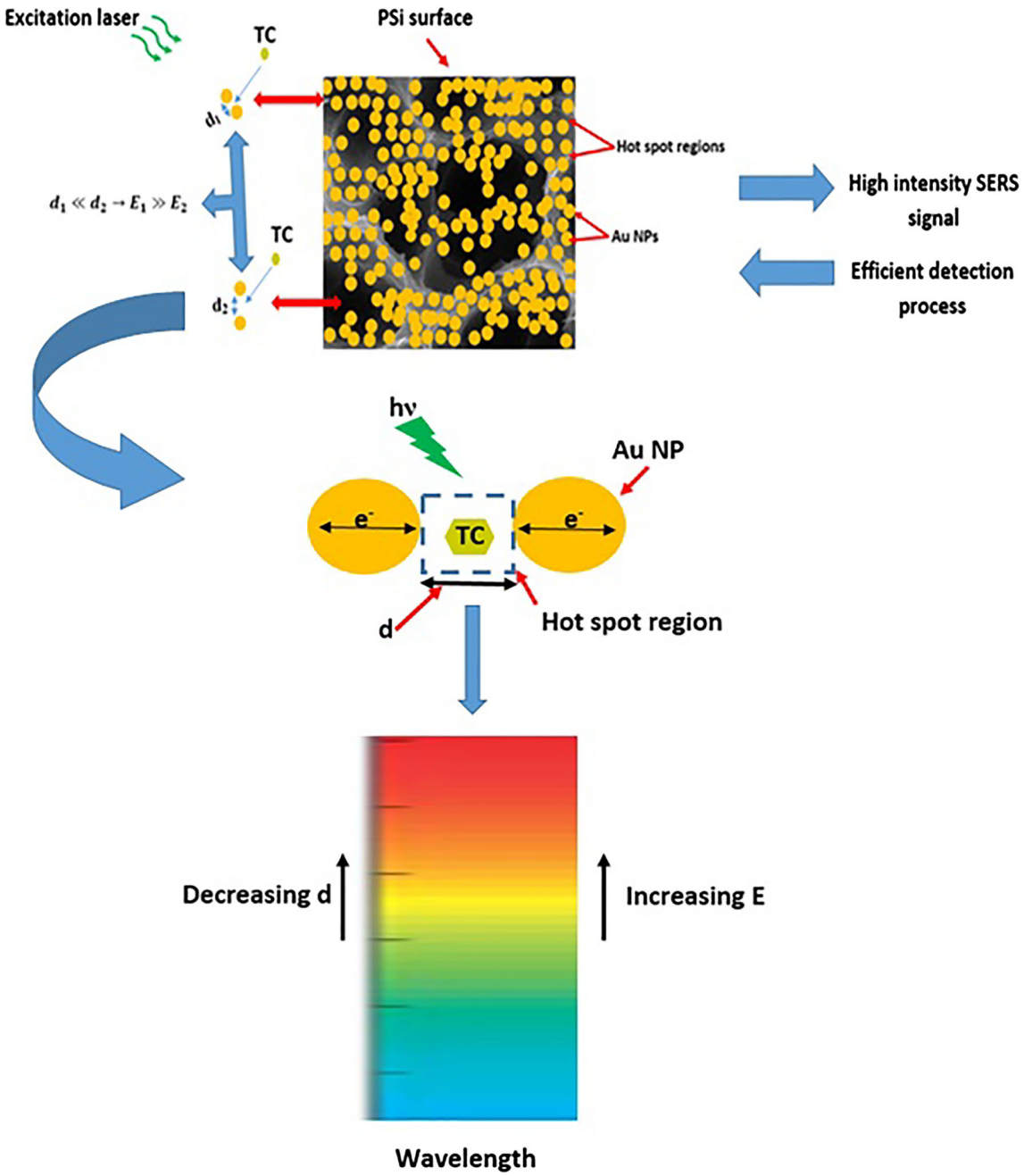

Fig. 2 The mechanism of the effect of the hot spot regions on the local electric field

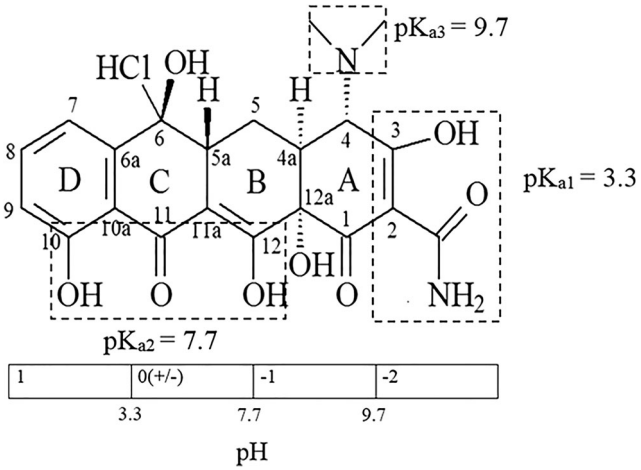

Fig. 3 The chemical structure of TC [28], and the pH-dependent speciation of tetracycline (TC) [29]

formed on the macroPSi surface through the Au ion reduction process by the Si-H dangling bonds of the surface of macroPSi as follows [25, 26]:

$$Si + 6HF \rightarrow H_2SiF_6 + 4H^+ + 4e^- \quad (1)$$

$$Au^{+3} + 3e^- \rightarrow A \quad (2)$$

Because the prepared macroPSi surface had a high density of dangling bonds (Si-H), the Au NPs was deposited on the surface of macroPSi in aggregated forms with a high density of hot spot regions, leading to synthesis of the Au NPS/macroPSi hot spot SERS sensor.

A standard stock solution of 0.1 mol/L TC was first prepared by dissolving 0.480 g of tetracycline dissolved in 10 mL ethanol, and then the solution was diluted with deionized water prepare TC aqueous solutions with low concentrations of 1×10^{-2}, 1×10^{-3}, 1×10^{-5}, 1×10^{-7}, and 1×10^{-9} mol/L. The solutions of TC with different pH values were obtained by adding NaOH or HCl to the 0.01 mol/L TC solution.

Characterization

The TESCAN MIRA3 field-emission scanning electron microscope (FE-SEM) was used for characterizing the morphologies of the bare macroPSi substrates and the deposited Au NPs on the macroPSi surfaces. The SERS efficiency was determined using aqueous solution of TC adsorbed on Au NPs/macroPSi hot spot SERS sensor. The sensor was immersed into these solutions at different low concentrations and various pH values for 10 h. The usual Raman and SERS spectra were measured by the APUS TESCAN Raman microscope, using a 532 nm DPSS ND: YAG (CW) laser for excitation with 10 mW laser excitation power and 3 s integration time.

Results and discussion

Morphological properties

The porosity, thickness layer, pore size, and the pore shape of the macroPSi substrate have very important roles in controlling the morphological properties of Au NPs deposited on the macroPSi surface. Thus, the optimum morphology of Au NPs can be achieved by choosing appropriate etching conditions. One can see in Fig. 1a, b, c, that the bare macroPSi substrate has been prepared with cylindrical pore shapes with sizes ranging from 0.25 to 2.25 μm and estimated porosity and thickness of 51.2% and 2.15 μm, respectively. Figure 1d,

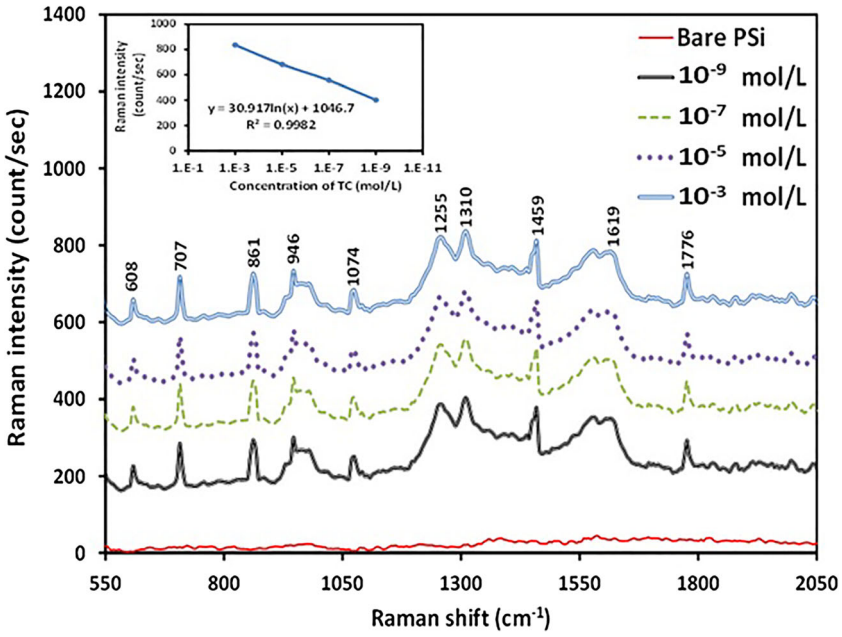

Fig. 4 The SERS spectra of the tetracycline aqueous solution at different concentrations of (10^{-3}–10^{-9} mol/L) for bare macroPSi and Au NPs/macroPSi hot spot sensor. The inset of this figure: the relation between the SERS intensity at highest peak of 1310 cm^{-1} and concentration of TC aqueous solution

e, f, which displays the FE-SEM of the Au NPs deposited on the surface of the prepared macroPSi, shows that the Au NPs were deposited on the pore walls (Fig. 1d). The high resolution image in Fig. 1e confirms that the morphology of the Au NPs deposited on the macroPSi consisted of irregular aggregates. This irregular form yields a high density of efficient hot spot SERS regions among the Au NPs. The size of the aggregated nanoparticles ranges from 25 to 225 nm, while the gaps among them (hot spot regions) ranges from 2.5 to 12.5 nm as shown in Fig. 1g, h, respectively. The high population (percentage) of small gaps of about 2.5 nm is considered to result in efficient hot spot regions due to the fact that the enhanced local electric field originating from these regions increased as the dimensions of the gaps decreased compared with the low percentage of Au NP sizes of about 225 nm. This can be expressed mathematically in the following equation [27], where, E_L represents the amplitude of the enhanced local electric field; d and D represent the sizes of hot spot regions and Au NPs, respectively.

$$E_L = E_i((d + D)/d) \quad (3)$$

The mechanism of the effect of hot spot regions on the local electric field is shown in schematic diagram Fig. 2. Figure 1i displays the energy dispersive X-ray spectroscopy (EDS) of the Au NPs/macroPSi hot spot sensor. This figure confirms the deposited of Au on the macroPSi surface and the presence of two other elements of *O* and Si.

SERS spectra of tetracycline antibiotic

The SERS spectra of the TC are related to the structure of TC. The chemical structure of tetracycline is composed of four rings of *D* (6a-7-8-9-10-10a-6a), *C* (5a-6-6a-10a-11-11a-5a), *B* (4a-5-5a-11a-12-12a-4a), and *A* (1–2–3-4-4a-12a-1), as shown in Fig. 3. The ring *D* is planar due to the double bonds of (*C*7 = *C*8, *C*9 = *C*10, and *C*6a = *C*10a). The sites (*C*9 to *C*12) which are located at the bottom half of the molecules are planar. The rings *C* and *B* are planar because both *C*6a = *C*10a-*C*11 = *O* and *O* = *C*11-*C*11a = *C*12 are coplanar with the ring *D*. The structure of ring *A* is nearly above the moiety plane (*C*9-*C*12) owing to the location of the *C*12a-OH and *C*4a-*H* sites below the plane, and *C*3 = *C*2-*C*1 = *O* is planar but not in the *C*9-*C*12 plane [28].

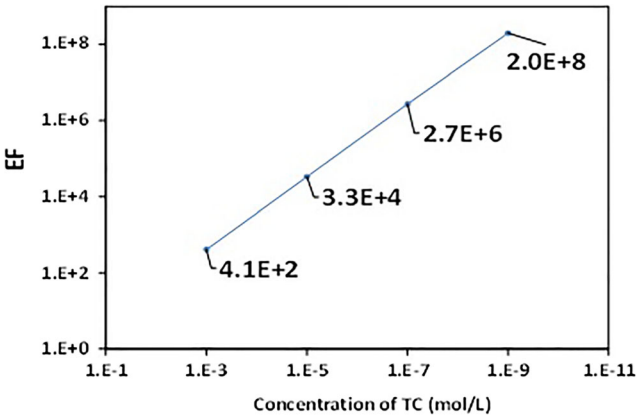

Fig. 5 The relation between EF and concentration of TC antibiotic

Figure 4 displays the SERS spectra of the tetracycline aqueous solution at different concentrations (10^{-3}, 10^{-5}, 10^{-7}, and 10^{-9} mol/L) for bare macroPSi and Au NPs/macroPSi hot spot SERS sensor. It is shown that the Raman signal of bare macroPSi is very weak compared with that of the Au NPs/macroPSi hot spot SERS sensor. And, the major tetracycline aqueous solution can be observed at positions 608, 707, 861, 946, 1074, 1255, 1310, 1459, 1579, 1619,

Table 1 The assignments of the SERS characteristic bands of TC antibiotic [2]

Raman shift (cm^{-1})	Assignments
608	Bending (amid-ONH)
707	out-of-plane swing (amin-NH), stretching(CO6,12), out-of-plane bending (OH3,6,10,12,12a)
861	Stretching(CO3)
946	Stretching(CO3)
1074	Stretching (CO6,12)
1255	Bending (CH4,4a,5a), bending (OH12), bending (amid-NH), stretching; (CO10), stretching; (CO3), stretching; (CH7,8.9), stretching; (amid-NC), stretching; (*C*4a*C*5), stretching (*D*)
1310	Bending(OH10,12), bending (CH 4,4a,5,5a), stretching (*C*5a*C*11a), stretching (*C*1*C*2), stretching(*C*9*C*10,*C*10*C*10a,*C*10a*C*11), stretching (CO11,12), (stretching CO3), bending(CH7,8,9)
1459	Bending(OH 10,12), stretching(*D*), stretching(*C*11a*C*12)
1619	Stretching (CO1), stretching (amid-CO), bending (amid-NH), stretching (CO3), stretching (*C*2*C*3), stretching (OH10,12), stretching (amid-CO_2)
1776	Stretching (CO1), stretching (amid-CO), bending (amid-NH), stretching (CO3), stretching (*C*2*C*3), stretching (OH10,12), stretching (amid-CO_2)

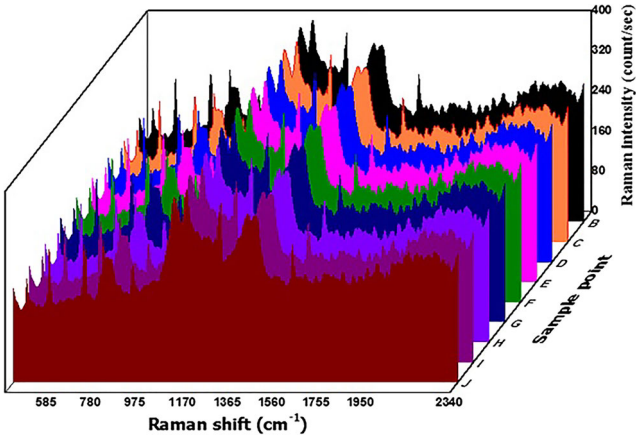

Fig. 6 The reproducibility of the SERS spectra for TC antibiotic

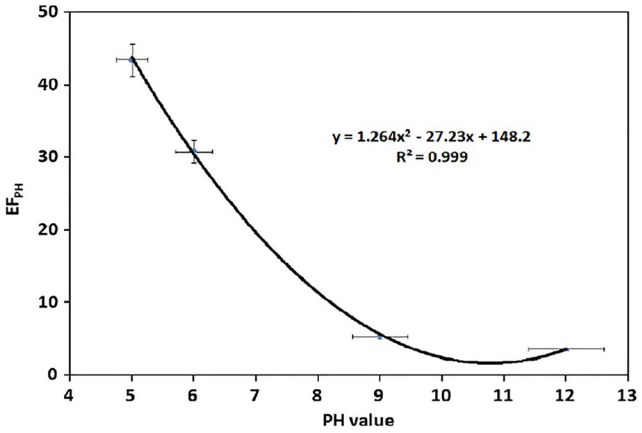

Fig. 8 The EF_{pH} versus pH values

1776, 1831, 1881, and 1995 cm^{-1}. According to the reference [4], the peaks of the tetracycline hydrochloride powder are located at 455, 497, 605, 709, 859, 945, 1073, 1136, 1285, 1317, 1462, 1632, and 1777 cm^{-1}. So, the peaks are at 608, 707, 861, 946, 1074, 1255, 1310, 1459, 1619, and 1776 cm^{-1} can be compared with that of the tetracycline hydrochloride powder, and can be selected as the characteristic peaks of SER for the detection of tetracycline aqueous solution using the Au NPs/macroPSi hot spot SERS sensor. The assignments of the SERS characteristic bands shown in Fig. 4 are listed in Table 1. It is found that the Raman signals are very strong for TC antibiotic adsorbed on the Au NPs/macroPSi hot spot sensor. The inset of Fig. 4 displays the relation between the intensity of SERS at the highest peak 1310 cm^{-1} and concentration of TC aqueous solution, where it can be seen that the relationship between them can be described by the following logarithmic equation: $y = 30.917 \ln(x) + 1046.7$ with a correlation coefficient (R^2) of (0.9982). The EF was determined by using the following equation for evaluating the lowest detection limit of the TC antibiotic [22], where, I_{SERS}, I_R are the signal intensities of the SERS and Raman, at the TC concentration of C_{SERS} and C_R, respectively.

$$EF = (I_{SERS} \times C_R)/(I_R \times C_{SERS}) \quad (4)$$

The relation between EF and the concentration of TC antibiotic is manifested in Fig. 5, the base line is the intensity of the bare PSi at wave number 1310 cm^{-1}. The EF value depended on the contribution of TC in the aqueous solution, which varied from 4.1×10^2 to 2.0×10^8, to a maximum value at a TC concentration of 10^{-9} mol/L. This means that the TC concentration of 10^{-9} mol/L is the minimum detection limit of the TC antibiotic. The detection process of TC antibiotic is at the lowest concentration with a higher value of EF (2.0×10^8), due to the plasmonic properties of Au NPs which enhanced as the density of the hot spot SERS increased.

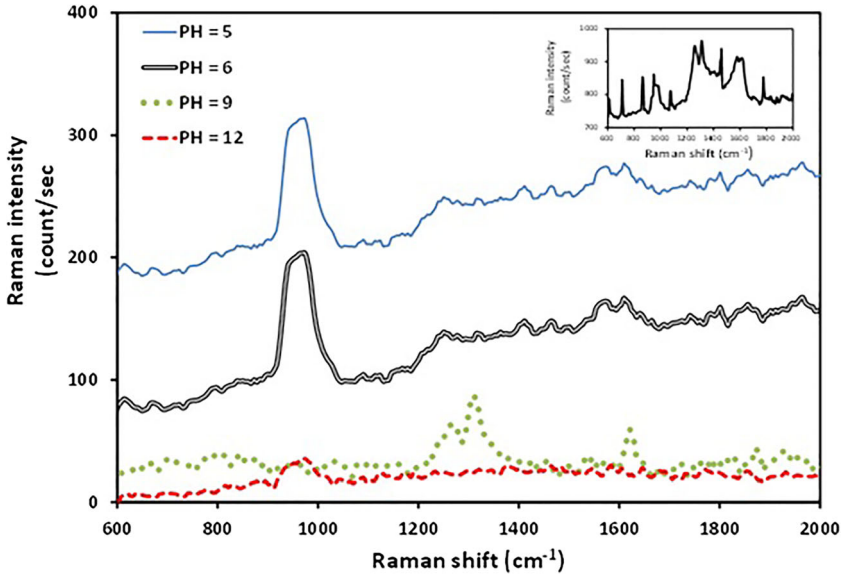

Fig. 7 The SERS curves of the TC aqueous solutions at 0.02 mol/L before (natural state) and after additional process of HCl or NaOH. The inset of figure display the natural state

To study the reproducibility of SERS spectra with the Au NPs/macroPSi hot spot SERS sensor for the detection process of TC antibiotic, the SERS spectra were examined at a number of points on the Au NPs/macroPSi hot spot SERS sensor surface at the lowest concentration of 10^{-9} mol/L. The reproducibility of these spectra for TC antibiotic is shown in Fig. 6. From this figure and the lowest value of the relative standard deviation for the SERS intensities of 2%, it was concluded that the Au NPs/macroPSi hot spot SERS sensor has excellent reproducibility.

The effect of pH value on the TC adsorbed on Au NPs/macroPSi hot spot SERS sensor

Figure 7 presents the SERS curves of the TC aqueous solutions at 0.02 mol/L before (natural state) and after the additional process of HCl or NaOH, respectively, revealing the relation between the pH of TC solution and behavior of the SERS curves. It is clearly shown that the behaviors of the curves change after the additional process of pH, and they are varied with the pH values, except that when the pH values are equal 5 and 6, the two curves behave in the same way. Also, the Raman signal intensity decreases after additional process and with increasing of pH values. The results demonstrated that the pH value of the TC solution is one of the most significant parameters affecting the adsorption process of the TC solution on the Au NPs/macroPSi hot spot SERS sensor. This can be attributed to the finding of three ionizable groups of the TC antibiotic, including, carboxymethyl at pK_a of 3.3, phenolic diketone at pK_a of 7.68, and dimethylamine cation at pK_a of 9.69. Thus, the changing of the pH values leads to the existence of TC in the solution as positively charged species (TCH_3^+) at the value of pH < 3.3 and as a zwitterion (TCH_2^0) at 3.3 < pH value < 7.7, while it exists in the solution as negatively charged species (TCH^- or TC^{2-}) when the pH value > 7.7 [29]. In addition, when 3.3 > pH value > 7.7, the TC is unstable and can form reversible epimers [30]. Therefore, the behavior of the SERS curves at the pH values of 9 and 12 changes, and the intensity of Raman signal is very small. Because the TC solution is predominantly neutral at 3.3 < pH value < 7.7, the SERS curves at the pH values of 5 and 6 have the same behavior and a higher Raman signal intensity. And, in spite of the behavior of these two curves differing compared with that at the natural state, they have several SERS bands, and can be compared with those at the natural state, including 614, 672, 974, 1091, 1255, 1320, and 1464 cm^{-1}. Thus, the pH values of 5 and 6 are the best for the detection process of TC antibiotic adsorbed on the Au NPs/macroPSi hot spot SERS sensor based on SERS as compared with the other values. Wali et al. [26] reported that the study of the pH influence on the SERS intensity can be satisfied by calculating the EF of SERS intensity for analyte under acidic and alkaline conditions, which is denoted as EF_{pH} by using the following equation:

$$EF_{pH} = I_{SERS}/I_R \quad (5)$$

Figure 8 shows the various EF_{pH} and pH values, it was found that the relationship between the EF_{pH} and the pH values is defined by the polynomial equation $y = 1.2643x^2 - 27.233x + 148.26$ with R^2 of 0.9997, so the highest and lowest EF_{pH} were obtained at the pH values of 5 and 12, respectively.

Conclusions

In summary, an efficient and highly rapid detection process has been innovated for detecting the residual TC antibiotic in water. The Au NPs/macroPSi hot spot sensor was developed through deposition process of Au NPs on the macroPSi surface with a high density of hot spot regions. The results elucidated that the Au NPs/macroPSi hot spot SERS sensor successfully provided chemical information for diagnosing the TC antibiotic with a high EF and reproducibility at ultra-low concentration of 10^{-9} mol/L. It was observed that the pH values of 5 and 6 are the best for the detection process of TC antibiotic adsorbed on the Au NPs/macroPSi hot spot SERS sensor based on SERS as compared with the other pH values of 9 and 12.The results proved that the Au NPs/macroPSi hot spot sensor is an excellent detection tool that can be used for qualitative and quantitative detection of TC residues in wastewater, and then for safety control.

Acknowledgments The authors would like to thank University of Technology, Baghdad-Iraq and Mustansiriyah University (www.uomustansiriyah.edu.iq), Baghdad-Iraq for their support in the present work.

Compliance with ethical standards

Conflict of interest The authors declare that they have no conflict of interest.

References

1. Connell SR, Tracz DM, Nierhaus KH, Taylor DE (2003) Ribosomal protection proteins and their mechanism of tetracycline resistance. Antimicrob Agents Chemother 47(12):3675–3681
2. Jin D, Bai Y, Chen H, Liu S, Chen N, Huang J, Huang S, Chen Z (2015) SERS detection of expired tetracycline hydrochloride with an optical fiber nano-probe. Anal Methods 7(4):1307–1312
3. Chopra I, Roberts M (2001) Tetracycline antibiotics: mode of action, applications, molecular biology, and epidemiology of bacterial resistance. Microbiol Mol Biol Rev 65(2):232–260
4. Dhakal S, Chao K, Huang Q, Kim M, Schmidt W, Qin J, Broadhurst CL (2018) A simple surface-enhanced Raman

spectroscopic method for on-site screening of tetracycline residue in whole Milk. Sensors 18(2):424
5. Gao Y, Li Y, Zhang L, Huang H, Hu J, Shah SM, Su X (2012) Adsorption and removal of tetracycline antibiotics from aqueous solution by graphene oxide. J Colloid Interface Sci 368(1):540–546
6. Lin Y, Xu S, Li J (2013) Fast and highly efficient tetracyclines removal from environmental waters by graphene oxide functionalized magnetic particles. Chem Eng J 225:679–685
7. Li R, Zhang H, Chen Q-W, Yan N, Wang H (2011) Improved surface-enhanced Raman scattering on micro-scale Au hollow spheres: synthesis and application in detecting tetracycline. Analyst 136(12):2527–2532
8. Hamscher G, Sczesny S, Höper H, Nau H (2002) Determination of persistent tetracycline residues in soil fertilized with liquid manure by high-performance liquid chromatography with electrospray ionization tandem mass spectrometry. Anal Chem 74(7):1509–1518
9. Zhang Y, Lu S, Liu W, Zhao C, Xi R (2007) Preparation of anti-tetracycline antibodies and development of an indirect heterologous competitive enzyme-linked immunosorbent assay to detect residues of tetracycline in milk. J Agric Food Chem 55(2):211–218
10. Burkhead MS, Wang H, Fallet M, Gross EM (2008) Electrogenerated chemiluminescence: an oxidative-reductive mechanism between quinolone antibiotics and tris (2, 2′-bipyridyl) ruthenium (II). Anal Chim Acta 613(2):152–162
11. Dang PK, Degand G, Danyi S, Pierret G, Delahaut P, Ton VD, Maghuin-Rogister G, Scippo M-L (2010) Validation of a two-plate microbiological method for screening antibiotic residues in shrimp tissue. Anal Chim Acta 672(1–2):30–39
12. Deng B, Xu Q, Lu H, Ye L, Wang Y (2012) Pharmacokinetics and residues of tetracycline in crucian carp muscle using capillary electrophoresis on-line coupled with electrochemiluminescence detection. Food Chem 134(4):2350–2354
13. Conzuelo F, Campuzano S, Gamella M, Pinacho DG, Reviejo AJ, Marco MP, Pingarrón JM (2013) Integrated disposable electrochemical immunosensors for the simultaneous determination of sulfonamide and tetracycline antibiotics residues in milk. Biosens Bioelectron 50:100–105
14. Song E, Yu M, Wang Y, Hu W, Cheng D, Swihart MT, Song Y (2015) Multi-color quantum dot-based fluorescence immunoassay array for simultaneous visual detection of multiple antibiotic residues in milk. Biosens Bioelectron 72:320–325
15. Chen Y, Chen Q, Han M, Liu J, Zhao P, He L, Zhang Y, Niu Y, Yang W, Zhang L (2016) Near-infrared fluorescence-based multiplex lateral flow immunoassay for the simultaneous detection of four antibiotic residue families in milk. Biosens Bioelectron 79:430–434
16. Li H, Chen Q, Hassan MM, Chen X, Ouyang Q, Guo Z, Zhao J (2017) A magnetite/PMAA nanospheres-targeting SERS aptasensor for tetracycline sensing using mercapto molecules embedded core/shell nanoparticles for signal amplification. Biosens Bioelectron 92:192–199
17. Watanabe K, Tanaka E, Ishii H, Nagao D (2018) The plasmonic properties of gold nanoparticle clusters formed via applying an AC electric field. Soft Matter 14(17):3372–3377
18. Lee J-H, Cho H-Y, Choi H, Lee J-Y, Choi J-W (2018) Application of gold nanoparticle to plasmonic biosensors. Int J Mol Sci 19(7): 2021
19. Alwan AM, Naseef IA, Dheyab AB (2018) Well controlling of plasmonic features of gold nanoparticles on macro porous silicon substrate by HF acid concentration. Plasmonics:1–9
20. Alwan AM, Dheyab AB (2017) Room temperature CO2 gas sensors of AuNPs/mesoPSi hybrid structures. Appl Nanosci 7(7):335–341
21. Petryayeva E, Krull UJ (2011) Localized surface plasmon resonance: nanostructures, bioassays and biosensing—a review. Anal Chim Acta 706(1):8–24
22. Alwan AM, Wali LA, Yousif AA (2018) Optimization of AgNPs/mesoPS active substrates for ultra-low molecule detection process. Silicon:1–11
23. Alwan AM, Yousif AA, Wali LA (2017) A study on the morphology of the silver nanoparticles deposited on the n-type porous silicon prepared under different illumination types. Plasmonics:1–9
24. Alwan AM, Yousif AA, Wali LA (2017) The growth of the silver nanoparticles on the mesoporous silicon and macroporous silicon: a comparative study. Indian J Pure Appl Phys (IJPAP) 55(11):813–820
25. Wali LA, Alwan AM, Dheyab AB, Hashim DA (2019) Excellent fabrication of Pd-Ag NPs/PSi photocatalyst based on bimetallic nanoparticles for improving methylene blue photocatalytic degradation. Optik 179:708–717
26. Wali LA, Hasan KK, Alwan AM (2019) Rapid and highly efficient detection of ultra-low concentration of penicillin G by gold nanoparticles/porous silicon SERS active substrate. Spectrochim Acta A Mol Biomol Spectrosc 206:31–36
27. Gunnarsson L, Bjerneld E, Xu H, Petronis S, Kasemo B, Käll M (2001) Interparticle coupling effects in nanofabricated substrates for surface-enhanced Raman scattering. Appl Phys Lett 78(6):802–804
28. Leypold CF, Reiher M, Brehm G, Schmitt MO, Schneider S, Matousek P, Towrie M (2003) Tetracycline and derivatives—assignment of IR and Raman spectra via DFT calculations. Phys Chem Chem Phys 5(6):1149–1157
29. Liu M, Hou L-a YS, Xi B, Zhao Y, Xia X (2013) MCM-41 impregnated with a zeolite precursor: synthesis, characterization and tetracycline antibiotics removal from aqueous solution. Chem Eng J 223:678–687
30. Liu D, Song N, Feng W, Jia Q (2016) Synthesis of graphene oxide functionalized surface-imprinted polymer for the preconcentration of tetracycline antibiotics. RSC Adv 6(14):11742–11748